IOSR Journal of Applied Physics (IOSR-JAP)
e-ISSN: 2278-4861.Volume 18, Issue 4 Ser. 1 (Jul. – Aug. 2026), PP 36-40
www.iosrjournals.org

Rotational temperature of GaCl from the $A^3\Pi_0^+ - X^1\Sigma^+$ and $B^3\Pi_1 - X^1\Sigma^+$ systems: a parallel/perpendicular consistency test

S. N. Adik
a Department of Physics, Shri Dnyaneshwar Mahavidyalaya, Newasa, Ahmednagar 414603, India

Abstract
We measured individual rotational-line intensities in the high-resolution Fourier-transform emission spectrum of $^{69}Ga^{35}Cl$ between 28 000 and 30 000 cm^{-1}. The spectrum was recorded from an electrodeless microwave discharge at an apodised resolution of 0.035 cm^{-1}. Profile integration yielded 1 381 unblended lines: the (0,0), (2,1), and (3,2) bands of the $A^3\Pi_0^+ - X^1\Sigma^+$ system, and the (0,0), (0,1), (0,2), and (1,2) bands of $B^3\Pi_1 - X^1\Sigma^+$. Although the two systems share a lower state, their symmetries differ. A-X is a 0^+-0^+ transition with $\Delta\Omega = 0$, while B-X is perpendicular with $\Delta\Omega = 1$; each therefore requires its own Hönl-London factors. Separate analyses gave T_{rot} = 1657 ± 41 K and 1691 ± 38 K. These values agree within their uncertainties, and the weighted mean of all eighteen branch data sets is 1676 ± 28 K. This agreement is significant because the two upper states are populated independently and analysed under different selection rules. No rotational temperature has previously been derived for GaCl from the A-X system.

Keywords: *GaCl; Fourier transform spectroscopy; rotational temperature; Hönl-London factors; group IIIA monohalides*

Date of Submission: 10-08-2026 Date of Acceptance: 22-08-2026

I. Introduction

Group IIIA monohalides have been studied for several decades. Some show bound-free transitions favourable to laser action [1,2], and their strong emission in low-pressure discharges also makes them useful source diagnostics. Gallium monochloride is among the better characterised members of this group. Its ultraviolet emission contains two overlapping, violet-degraded systems, $A^3\Pi_0^+ - X^1\Sigma^+$ and $B^3\Pi_1 - X^1\Sigma^+$. Several groups have analysed these systems at progressively higher resolution [3-6]. The most recent study, by Saksena et al. [7], provides the line positions and J assignments used here. Singh [8] compiled the molecular constants of all four gallium monohalides.

Most previous work has concentrated on line positions. Intensities provide different information: they show how the population is distributed over the rotational manifold and therefore indicate the temperature of the emitting gas. This information had not been extracted for GaCl. We previously reported a preliminary value from two P branches [9]. The present paper supersedes that result by using the complete data set, corrected line-strength factors, and properly propagated uncertainties.

The two systems provide a particularly useful consistency test. $A^3\Pi_0^+ - X^1\Sigma^+$ is a parallel transition with $\Delta\Omega = 0$, whereas $B^3\Pi_1 - X^1\Sigma^+$ is perpendicular with $\Delta\Omega = 1$. Both were recorded from the same discharge and share the same lower state, so they should yield the same rotational temperature when the appropriate line-strength factors are used.

II. Experimental

The spectra are those reported by Saksena et al. [7], so only the essential experimental details are repeated here. GaCl was excited in an electrodeless microwave discharge lamp operated at 2450 MHz and 180 W, with a flowing mixture of gallium chloride vapour and helium. A spherical lens focused the emission into a BOMEM DA8 Fourier-transform spectrometer equipped with a quartz ultraviolet beam splitter, a photomultiplier, and an order-sorting filter. The region from 28 000 to 30 000 cm^{-1} was recorded at an apodised resolution of 0.035 cm^{-1}, with sixty scans co-added. Only the $^{69}Ga^{35}Cl$ isotopologue was included in the analysis.

Two features of the FT measurement are important for the intensity analysis. First, the photomultiplier response is linear over the range used, so no equivalent of a photographic emulsion's characteristic-curve calibration is required. Second, each band covers a narrow interval, making any residual wavenumber dependence of the instrument response too small to affect a fit within that band. The spectrum was recorded in fragments on a fixed intensity scale, which allows measurements from different fragments to be compared directly.

Line profiles were digitised in Origin, and the area under each profile was taken as the line intensity. Every area was read several times with a digital planimeter, after which the mean was used. Lines overlapped by neighbouring features from either system were discarded. This left 1 381 usable lines: 586 in the three A-X bands and 795 in the four B-X bands.

III. Method of analysis

For an emission line connecting J′ in the upper state with J″ in the lower state, the integrated intensity is

$$I(J',J'') = A\, S(J',J'')\, \exp[- F_{v'}(J')\, hc / kT] \qquad (1)$$

Here A contains the factors independent of J, S(J′,J″) is the Hönl-London factor, and $F_{v'}(J') = B'_{v'}\, J'(J'+1) - D'_{v'}\, J'^2(J'+1)^2$ is the rotational term value of the upper state. The centrifugal term is negligible over the J range considered and is therefore omitted. Taking logarithms gives

$$- \ln [\, I(J',J'') / S(J',J'') \,] = \text{const.} + (hc / kT)\, B'_{v'}\, J'(J'+1) \qquad (2)$$

Thus, a plot of -ln(I/S) against $B'_{v'}\, J'(J'+1)$ should be linear, with slope hc/kT. Because the rotational constant is already included in the abscissa, it must not be introduced a second time. The temperature is then

$$T = (hc / k) / \text{slope} = 1.438777 / \text{slope} \quad K \qquad (3)$$

The upper-state rotational constants were calculated from $B'_{v'} = B'_e - \alpha'_e(v' + ½)$, using the values reported in Ref. [7].

3.1. Hönl-London factors and the role of Ω

The two electronic systems require separate Hönl-London expressions because their transition symmetries are different.

The $B^3\Pi_1$ - $X^1\Sigma^+$ transition is perpendicular: Λ′ = 1, Λ″ = 0, and ΔΩ = 1. For Λ″ = 0, Herzberg's expressions [10] for ΔΛ = ±1 reduce to

$$S_P = (J'' - 1)/4 , \quad S_Q = (2J'' + 1)/4 , \quad S_R = (J'' + 2)/4 \qquad (4)$$

The $A^3\Pi_{0^+}$ - $X^1\Sigma^+$ transition is different. The A state has $\Omega = 0^+$ and the ground state is $^1\Sigma^+$, so ΔΩ = 0 and the transition is parallel. For a 0^+-0^+ transition, ΔJ = 0 is forbidden; consequently, none of the A-X bands contains a Q branch. The appropriate strengths are those of a Σ-Σ transition:

$$S_P = J'' , \quad S_R = J'' + 1 \qquad (5)$$

These replace the perpendicular expressions in Eq. (4). Over the observed J range, the ratio between the two sets changes only slowly, so the fitted slope changes by about 1%. The numerical effect is small, but the distinction is physical. Using Eq. (5) for A-X and Eq. (4) for B-X is essential to a valid comparison of the two systems.

IV. Results

Table 1 summarises the separate branch fits. Each entry gives the number of lines, the J″ range, the upper-state rotational constant, the fitted slope and its standard error, the correlation coefficient, and the resulting rotational temperature.

Table 1. Rotational temperatures of GaCl from individual branches.

System	Band	Branch	N	J″ range	$B'_{v'}$ (cm^{-1})	slope ×10^{-4}	σ ×10^{-4}	r	T_{rot} (K)
A-X	(0,0)	P	126	26-161	0.157959	8.636	0.423	0.878	1666 ± 82
A-X	(0,0)	R	172	10-187	0.157959	8.714	0.297	0.914	1651 ± 56
A-X	(2,1)	P	55	62-117	0.155859	8.611	1.571	0.601	1671 ± 305
A-X	(2,1)	R	84	51-137	0.155859	8.621	0.643	0.829	1669 ± 125
A-X	(3,2)	P	60	41-105	0.154809	8.572	1.612	0.573	1678 ± 316
A-X	(3,2)	R	89	31-124	0.154809	8.721	0.706	0.798	1650 ± 134
B-X	(0,0)	P	110	28-148	0.157582	8.532	0.632	0.793	1686 ± 125
B-X	(0,0)	Q	154	15-183	0.157582	8.493	0.214	0.955	1694 ± 43
B-X	(0,0)	R	89	19-120	0.157582	8.526	0.999	0.675	1688 ± 198
B-X	(0,1)	P	49	26-83	0.157582	8.609	2.718	0.419	1671 ± 528
B-X	(0,1)	Q	112	9-125	0.157582	8.590	0.923	0.664	1675 ± 180
B-X	(0,1)	R	48	19-68	0.157582	8.749	3.011	0.394	1644 ± 566
B-X	(0,2)	P	44	28-76	0.157582	8.560	2.796	0.427	1681 ± 549
B-X	(0,2)	Q	65	13-83	0.157582	8.580	1.444	0.599	1677 ± 282

System	Band	Branch	N	J″ range	$B'_{v'}$ (cm^{-1})	slope ×10^{-4}	σ ×10^{-4}	r	T_{rot} (K)
B-X	(0,2)	R	38	23-64	0.157582	8.630	5.276	0.263	1667 ± 1019
B-X	(1,2)	P	29	15-54	0.156532	8.735	10.108	0.164	1647 ± 1906
B-X	(1,2)	Q	30	32-64	0.156532	9.061	8.080	0.207	1588 ± 1416
B-X	(1,2)	R	27	33-59	0.156532	8.644	10.639	0.160	1665 ± 2049

The uncertainties in T_{rot} were propagated from the standard error of each fitted slope and describe only the internal precision of the corresponding fit.

Figure 1 shows Boltzmann plots for the (0,0) band of each system, while Fig. 2 brings together all eighteen temperature determinations.

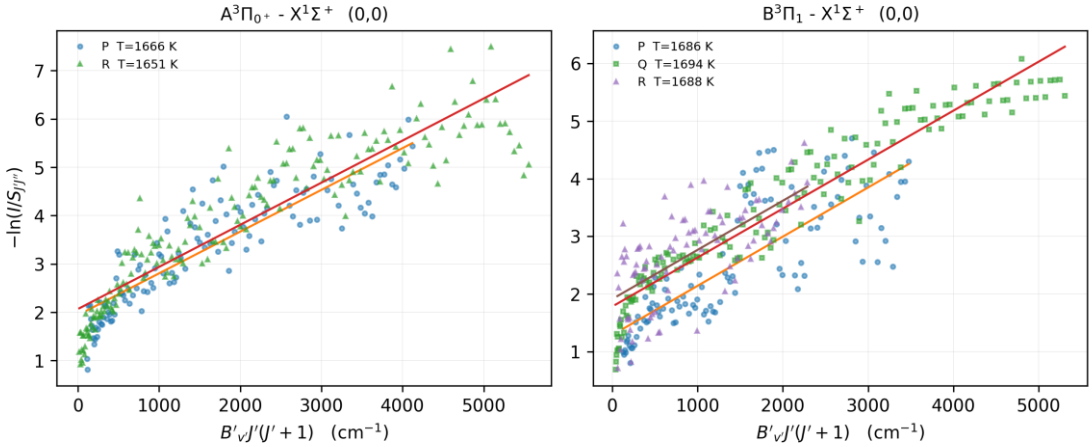

Fig. 1. Boltzmann plots for the (0,0) bands of the $A^3\Pi_{0^+}$ - $X^1\Sigma^+$ (left) and $B^3\Pi_1$ - $X^1\Sigma^+$ (right) systems of GaCl. Solid lines are least-squares fits to Eq. (2). The A-X system has no Q branch, as required by the 0^+-0^+ selection rule.

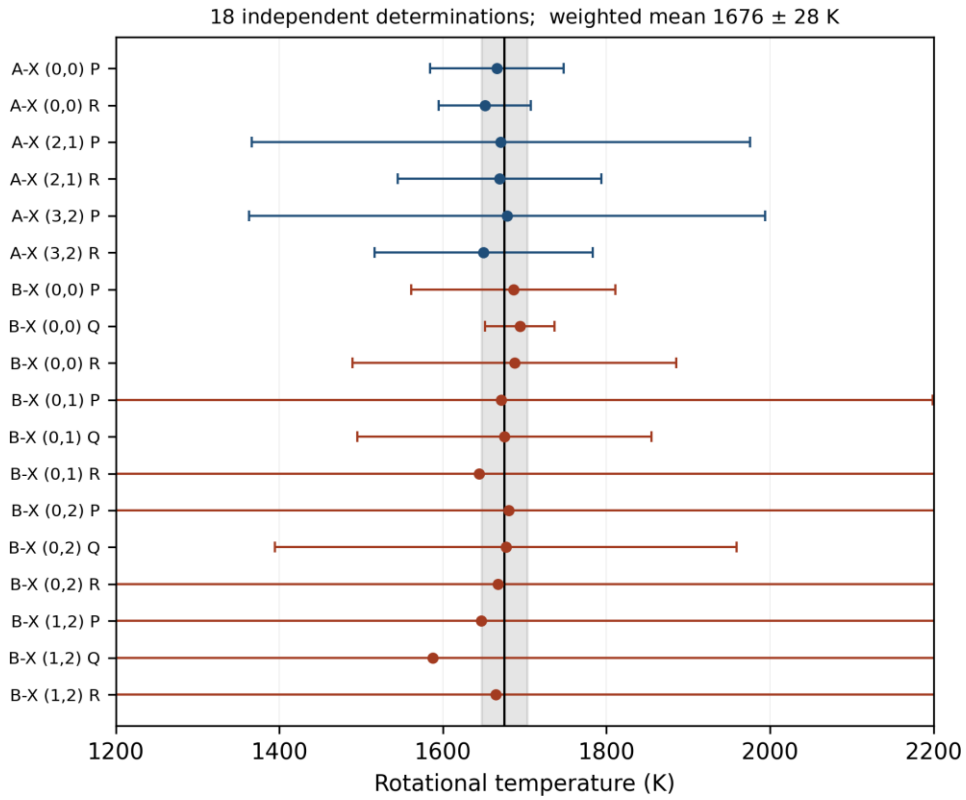

Fig. 2. The eighteen independent temperature determinations with their propagated uncertainties. The vertical line and shaded band show the weighted mean and its standard error, 1676 ± 28 K.

When the measurements are grouped by band system, the results are

$A^3\Pi_0^+ - X^1\Sigma^+$: $T_{rot} = 1657 \pm 41$ K (6 data sets)

$B^3\Pi_1 - X^1\Sigma^+$: $T_{rot} = 1691 \pm 38$ K (12 data sets)

The two values differ by 34 K, equivalent to 0.6 times the quadrature sum of their uncertainties. Combining all eighteen data sets gives a weighted mean of 1676 ± 28 K.

V. Discussion

5.1. The consistency test

The central result is the agreement between the two systems. A and B are separate electronic states, populated independently in the discharge, and their emission is analysed with different line-strength formulae. The common temperature supports the Ω assignment in Section 3.1, indicates that both upper-state rotational manifolds are in equilibrium with the same translational reservoir, and argues against a J-dependent intensity error large enough to bias the slope. If the perpendicular expressions in Eq. (4) were also used for A-X, its temperature would shift by roughly 10 K. That shift lies within the present uncertainty, but it would become more important for a wider J range or a cooler source.

5.2. Uncertainties

The internal uncertainties in Table 1 vary widely. They range from ±43 K for the strongest data set (154 lines, r = 0.955) to more than ±1000 K for the weakest (27 lines, r = 0.160). This spread is inherent in the method. The slope in Eq. (2) depends on the range of $J'(J'+1)$ sampled by a branch, so even carefully measured areas carry little weight when they cover only a short J interval. Data sets with fewer than about forty lines make a negligible contribution to the mean and are retained in Table 1 for completeness.

The eighteen values scatter much less than their individual uncertainties would suggest ($\chi^2/\nu = 0.03$), but this does not imply exceptional precision. All determinations share one spectrum, instrument, and operator, so any systematic error in the intensity scale is common to them. Their spread about the mean, ±6 K, measures the repeatability of the profile measurements and should not be quoted as the uncertainty in T_{rot}. We therefore take the weighted mean and its propagated error, 1676 ± 28 K, as a lower bound. Combining this with estimated systematic contributions of ±15 K from the line-strength choice and ±20 K from planimetry gives a final value of 1676 ± 40 K.

5.3. Data excluded from the analysis

The measured A-X (1,0) band was excluded from the final analysis. Neither branch showed any dependence on $J'(J'+1)$: the correlation coefficient was -0.022 for the 63 P-branch lines and -0.001 for the 91 R-branch lines, so no slope could be recovered. This band lies in a crowded region where B-X (0,1) lines overlap A-X (1,0) lines, suggesting that the original overlap criterion did not identify every blend. The two data sets have negligible weights and would not change the weighted mean, but they would distort an unweighted average; for that reason, they were omitted.

5.4. Physical significance

The measured quantity is a gas-kinetic rotational temperature, not the much lower temperature of the discharge tube. A value near 1700 K describes a comparatively cool source. At 29 000 cm^{-1}, the corresponding Doppler width is 0.083 cm^{-1}, slightly greater than the apodised instrumental resolution; the observed lines should therefore be Doppler limited. This is consistent with the sharp, well-separated contours and the clean P, Q, and R structure. A hotter source would populate levels near the dissociation limit at about 39 900 cm^{-1} [8] and would blur the band structure. We do not derive a vibrational temperature because the available bands span too narrow a range of v'.

VI. Conclusions

We measured intensities for 1 381 unblended rotational lines in the $A^3\Pi_0^+ - X^1\Sigma^+$ and $B^3\Pi_1 - X^1\Sigma^+$ systems of $^{69}Ga^{35}Cl$ and used them to determine the rotational temperature. With the line strengths appropriate to $\Delta\Omega = 0$ and $\Delta\Omega = 1$, the systems independently give 1657 ± 41 K and 1691 ± 38 K. Agreement between two upper states populated independently and analysed under different selection rules provides a check that a single band system cannot offer. The combined result is 1676 ± 28 K statistically, or 1676 ± 40 K when the estimated systematic contributions are included. This is the first GaCl rotational temperature derived from the A-X system and the first analysis to treat the Ω dependence of the line strengths explicitly.

References

[1] M. Singh, G. S. Ghodgaonkar, M. D. Saksena, J. Quant. Spectrosc. Radiat. Transfer (as cited in Ref. [8]).
[2] R. Venkatasubramanian, M. D. Saksena, M. Singh, Chem. Phys. Lett. 210 (1993) 367.
[3] M. D. Saksena, R. Venkatasubramanian, M. Singh, J. Mol. Spectrosc. 168 (1994) 290.
[4] M. D. Saksena, R. Venkatasubramanian, M. Singh, Can. J. Phys. 75 (1997) 191.
[5] E. Mahieu, I. Dubois, H. Bredohl, J. Mol. Spectrosc. 138 (1989) 264.
[6] M. D. Saksena, M. N. Deo, J. Mol. Spectrosc. 208 (2001) 64.
[7] M. D. Saksena, M. N. Deo, K. Sunanda, H. A. Khan, J. Mol. Spectrosc. 235 (2006) 166.
[8] V. B. Singh, J. Phys. Chem. Ref. Data 34 (2005) 23.
[9] S. Adik, C. T. Londhe, S. H. Behere, Int. J. Res. Biosci. Agric. Technol. 4 (2016) 119.
[10] G. Herzberg, Molecular Spectra and Molecular Structure I. Spectra of Diatomic Molecules, 2nd ed., Van Nostrand Reinhold, New York, 1950.
[11] K. P. Huber, G. Herzberg, Molecular Spectra and Molecular Structure IV. Constants of Diatomic Molecules, Van Nostrand Reinhold, New York, 1979.